

NUMERICAL AND PHYSICAL EXPERIMENTS ON SHEAR BANDING IN SANDSTONE

A. Fakhimi¹ and J.F. Labuz²

¹New Mexico Institute of Mining & Technology, Socorro 87801, USA & Tarbiat Modarres University, Tehran, Iran

²Department of Civil Engineering, University of Minnesota, Minneapolis 55455, USA

ABSTRACT

The development of a localized damage zone or shear band in rock was studied through numerical and physical experiments. A laboratory biaxial (plane strain) compression test was conducted on a prismatic specimen of Berea sandstone. The shear band initiation and propagation were monitored by locations of acoustic emission and examination of thin sections of the failed specimen. Numerical analysis using a discrete element model was conducted to simulate the laboratory results. The model was able to capture many details of the damage zone observed in the physical experiment.

1 INTRODUCTION

Plane-strain (biaxial) compression tests were conducted on rectangular prisms of Berea sandstone to study the initiation and propagation of a shear band (Labuz et al. [1]). The particular experiment reported in this work featured a specimen that contained an imperfection (a 3.5 mm diameter hole) to trigger localization from its central point. The experiment was performed with a closed-loop, servo-hydraulic loading system. The induced shear banding in the sandstone was studied through locations of acoustic emission. In addition, thin sections of the specimen, after completion of the laboratory test, were prepared and examined under an optical microscope, to study the nature of the primary and secondary fractures in the specimen.

Numerical modeling was also conducted to simulate shear banding in rock. The synthetic material used in the numerical analysis consisted of 2D rigid circular particles that interact through normal and shear springs. These disks were glued to each other through normal and shear bonds to be able to withstand the applied loads. An explicit discrete element technique was used to conduct the numerical modeling. CA2 computer program (Fakhimi [2]), which can simulate the interaction of a continuum and a discrete system, was utilized. Discrete element modeling of rock fracture has already been considered by several researchers. The main contribution of this numerical code, which differentiates it from those of previous investigators, is the use of a slightly overlapped circular particles interaction (SOCPI) algorithm in simulating failure. This model is capable of reproducing friction angles similar to real rock. In this study, progressive extension of the shear band was examined and compared to the physical experiment.

2 PHYSICAL EXPERIMENTS

A plane strain apparatus, similar to that of Vardoulakis and Goldscheider [3], was used to study failure of Berea sandstone. The apparatus was designed to allow a shear band to develop and propagate in an unrestricted manner by attaching a platen to a low friction linear bearing (Labuz et al. [1]). Plane-strain deformation is enforced by passive restraint (a thick-walled steel cylinder), and prismatic specimens are used. The Berea sandstone tested can be characterized by the following properties: $E = 14$ GPa, $\nu = 0.3$, uniaxial compressive strength $q_u = 40$ -50 MPa. The sandstone, 99% silica with 20% porosity, has an average grain size of 0.2 mm and slight anisotropy due to its sedimentary origin. Several specimens, 75-100 mm in length, 27-40 mm in width and 100 mm in thickness (in plane strain direction) were tested at confining pressures of 5, 10, and 20 MPa; an experiment at 5 MPa confinement is reported. The particular specimen was 99.30 mm high and 27.84 mm wide. The specimen contained a 3.4 mm diameter hole at its center that was drilled parallel to the plane strain direction. This imperfection was used to initiate failure at the specimen center. The axial load was measured with load cells mounted above and below the specimen. Axial and lateral deformations were monitored by four LVDTs. The average lateral displacement from two LVDTs was used as the feedback signal to control the failure process in the softening regime. The loading

was adjusted to achieve a 10^{-4} mm/s lateral displacement rate. The surfaces of the loading platens were covered with stearic acid to reduce frictional constraint at the boundaries.

Fig. 1a shows the mechanical response. The peak stress was 75.2 MPa, followed by a short period of stable softening. Significant snap-back behavior was observed (Fig. 1b), and at an axial stress of 61 MPa, about 81% of the peak stress, labeled “unc 1” in Fig. 1b, test control was momentarily lost and an abrupt unload occurred to an axial stress of 35.2 MPa. At this stress level, the loading system started correcting itself by trying to follow the command signal. Later on, at an axial stress of 45.2 MPa (60% of peak stress), with an audible sound of fracture, the failure process was uncontrolled again, labeled as “unc2” in Fig. 1b. The loading system eventually regained control and residual sliding was observed (Fig. 1a).

After the test, the specimen was removed from the biaxial test apparatus and the fracture pattern was inspected. The induced shear band consisted of a primary fracture in the middle and two kinked fractures close to the lateral boundaries of the specimen. The primary and kinked fractures were oriented 77° and 62° from the minor principal stress direction (Fig. 2a). The resultant displacement vector, calculated from the lateral and axial LVDTs during residual sliding, were oriented 70° from the minor principal stress direction.

2.1 Optical microscopy

Thin sections of the specimen were examined to study the nature of induced fracture more closely. To prepare the thin sections, the specimen at the end of the laboratory test was coated with epoxy glue and later potted in hydrostone. After cutting the specimen in half, the block was quenched in a low viscosity blue-colored epoxy to increase the visibility of porosity and to preserve the structure of the failure zone during thin section preparation. Four thin sections were examined under reflected light at magnification ranging from about 10x-50x. Photographs were taken with a digital camera mounted on the microscope.

Along the primary fracture, there was visual increase in porosity extending about 1-2 mm or 4-8 grain diameters to each side (Fig. 2b). The increase in porosity in the vicinity of the primary fracture can be attributed to the positive volumetric plastic strain or dilation due to shear movement. Along the secondary or kinked fractures that were less inclined to the direction of minimum compressive stress, less crushing of grains along the margins of the failure surface was observed, compared to that of primary fracture (Fig. 2b). In addition, there was no visual evidence for an alteration in porosity within margins of the kinked region. This lack of change of porosity along the kinked fracture could imply that the surface was formed by mixed mode deformation dominated by tensile fracture.

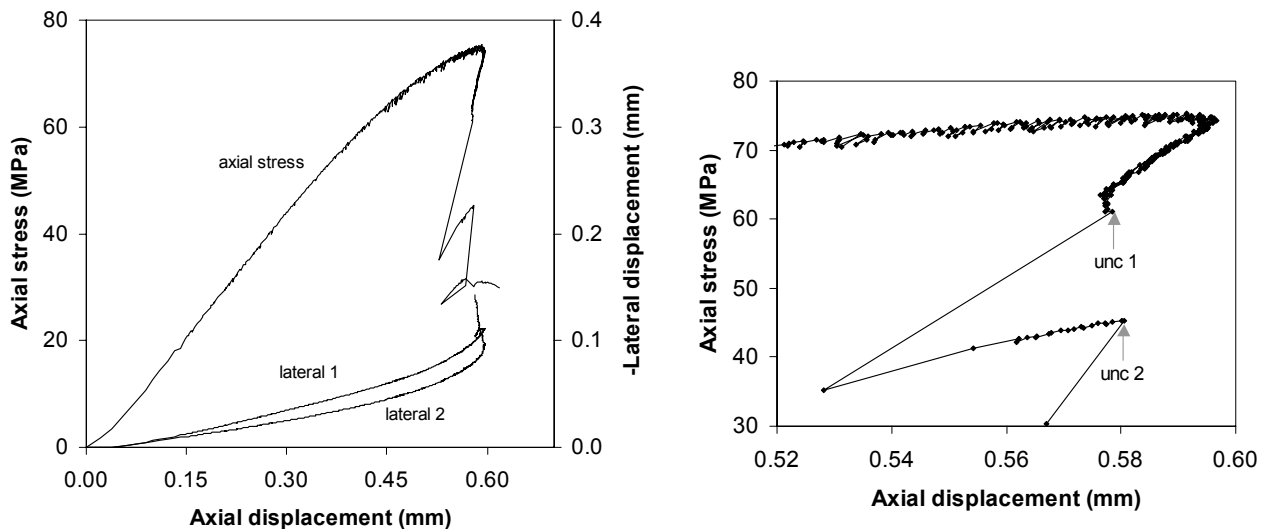


Figure 1: Results from the plane-strain compression tests on Berea sandstone at 5 MPa confinement. (a) Mechanical response. (b) Post-peak response.

Along the transition zone, at the location of primary and kinked fracture intersection, some interesting features were observed. Fig. 2b illustrates the transition zone, with the vertical line being parallel to the direction of maximum principal stress. As the primary fracture is followed close to the transition zone, the quantity of the crushed grains in the image decreases. Furthermore, at the end of primary fracture, a process zone can be observed, which has the same orientation as the main fracture with less damaged grains around its faces. The end zone of the primary fracture was most obvious in the thin section shown in Fig. 2c. In summary, the fracture in the specimen started from the hole boundary and propagated with further deformation of the specimen. This primary crack, with process zones at its ends, was eventually arrested. The kinked fractures were created afterward, apparently extending from the free lateral boundaries toward the transition zone. The boundary effect could have played a major role in deviation of the orientation of the primary fracture and development of kinked fractures.

3 NUMERICAL MODELING

An effort was made to simulate the laboratory biaxial test numerically. To this end, a slightly overlapped circular particle interaction (SOCPI) model through an explicit discrete element method was used. The detailed description of the SOCPI model can be found in Fakhimi [2]. In this model, 2D rigid circular particles are randomly generated, inflated and compacted by a hydrostatic stress σ_0 (genesis pressure) to create a well-packed conglomerate. The circular disks can interact through normal and shear springs. Due to non-zero genesis pressure (σ_0), slight overlaps are created between contacted disks. It has been shown that this small overlap can cause the synthetic material to show a more realistic friction angle and q_u/σ_t (ratio of unconfined compressive strength to tensile strength) values similar to rock. All numerical experiments were conducted using CA2 computer program. This program is capable of solving large deformation solid mechanics problems and the interaction of a continuum and a discrete system such as a SOCPI model. Therefore, with this program, the surrounding walls around the disk assemblage were discretized to finite elements and hence they were deformable.

Fakhimi and Villegas [4] used dimensional analysis for a SOCPI model and introduced non-dimensional graphs for calibration of a synthetic material for Young's modulus, Poisson's ratio, Mohr-Coulomb failure envelope and tensile strength of the rock. These graphs can be used for calibration of a SOCPI model. The following parameters were obtained for the synthetic material similar to Berea sandstone: $K_n = 32$ GPa, $K_s = 5$ GPa, $\mu = 0.5$, $n_b = 4600$ N/m, $s_b = 28000$ N/m, $\sigma_0 / K_n = 0.04$, $R = 0.2$ mm, where R is the average disk radius. Numerical experiments on specimens of this synthetic material, 75 mm high and 30 mm wide were conducted to obtain the macroscopic properties of the model: $E = 14.8$ GPa, $\nu = 0.24$, $q_u = 49.4$ MPa. These compare well with those of the Berea sandstone tested.

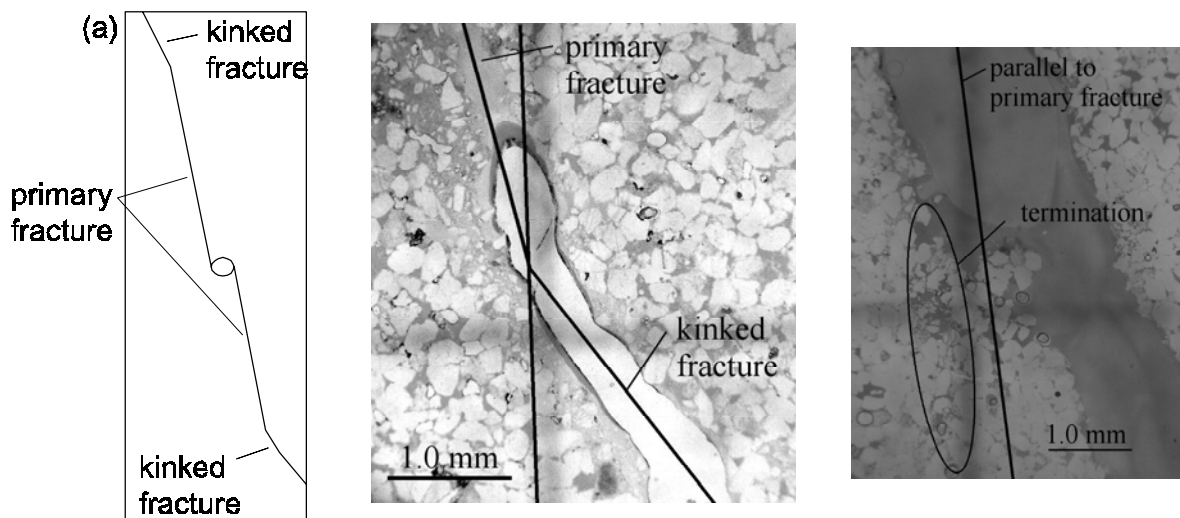


Figure 2: (a) Sketch of specimen failure. (b) Transition zone of failure surface. (c) Evidence of a process zone.

A specimen of the synthetic material similar to Berea sandstone was tested numerically. The specimen's dimensions (27.84×99.3 mm) were the same as that of the Berea sandstone specimen. A hole of 3.4 mm in diameter was excavated from the center of the specimen before any external loads were applied. Initially, a confining pressure of 5 MPa was applied to the flexible lateral boundaries (lateral walls). Through numerical cycling, the applied pressure was transferred to the synthetic material. After equilibrium, the lower wall was fixed vertically and the upper wall was moved downward with a constant velocity of 0.5×10^{-5} mm/cycle. A microcrack in CA2 is illustrated by a line segment perpendicular to the line connecting the center of two disks with a broken bond.

The mechanical response of the numerical specimen is shown in Fig. 3a, which compares well to Fig. 1a. The strength of the synthetic material was 84.4 MPa, 12% higher than that for the sandstone. This could be due to approximation in the numerical modeling or due to heterogeneity that is inevitable in a natural stone. Recall that the Berea sandstone tested had an unconfined compressive strength with a range of 40-50 MPa. Other than the approximation in the predicted peak stress, the axial stress-displacement curve is similar to that for Berea sandstone. The lateral deformation of the synthetic material due to the applied deviatoric stress is also shown in Fig. 3a. These lateral displacement-axial displacement curves for right and left specimen boundaries are similar to those for sandstone, although a relatively greater dilation can be seen for the synthetic specimen. Initially, the curve of lateral-axial displacement was linear with a slope that is proportional to the Poisson's ratio of the specimen. Later on by further deformation of the specimen and development of new cracks, the slope of the curve increased. Finally, a drastic increase in lateral deformation occurred at the peak stress. This is qualitatively consistent with that in the laboratory test (Fig. 1a).

Fig. 3b shows the damage zones in the specimen at peak stress, at the beginning of the softening regime. Damage zones in this figure are shown through the broken bonds (lighter regions) between adjacent disks initially in contact, which have become separated due to excessive slip or dilation. From the axial stress of 25 MPa (microcrack initiation stress) to 84.4 MPa (peak stress), many microcracks were developed in the specimen but no localization along a shear band was observed. In Fig. 3b, a macroscopic fracture is visible at the upper-right side of the hole. This damage zone was steep, similar to the primary fracture in the laboratory test. Figs. 3c-e show the extension of damage zones around four points of the imperfection at the axial stresses of 81.1, 79.5 and 77.5 MPa, i.e. at 96%, 94% and 89% of the peak stress in the post-peak regime. It is evident from these figures that only the upper right and lower left damage zones extended by further deformation of the specimen. It is also realized that the secondary or kinked damaged zone was gradually developed in the upper-right region of the specimen.

Acknowledgement—Partial support was provided by NSF grant number CMS-0070062.

REFERENCES

1. Labuz J.F., Dai S-T., Papamichos E. Plane-strain compression of rock-like materials. *Int. J. Rock Mech. Min. Sci. Geomech. Abstr.* 33:573-584. 1996.
2. Fakhimi A. Application of slightly overlapped circular particles assembly in numerical simulation of rocks with high friction angle. *J. Engng. Geol.* In press. 2004.
3. Vardoulakis I., Goldscheider M. Biaxial apparatus for testing shear bands in soils. *Proc. 10th Int. Conf. Soil Mech. Found. Engng.* Balkema, Rotterdam, 819-824. 1981.
4. Fakhimi A., Villegas T. Calibrating a discrete element model for rock failure envelope and tensile strength. *Proc. 2nd Int. PFC Symp*, Kyoto, Japan. To be submitted. 2004.

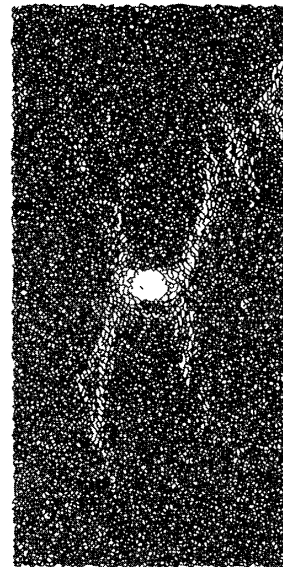
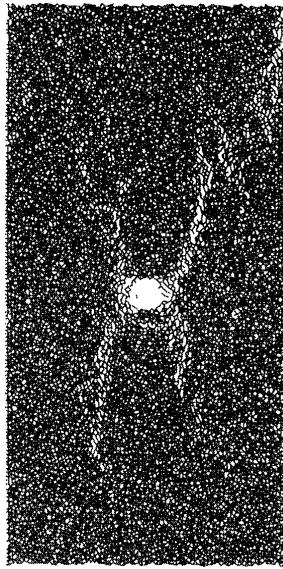
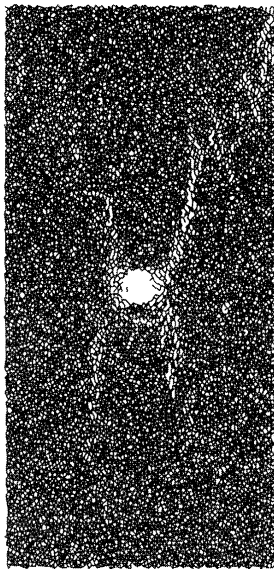
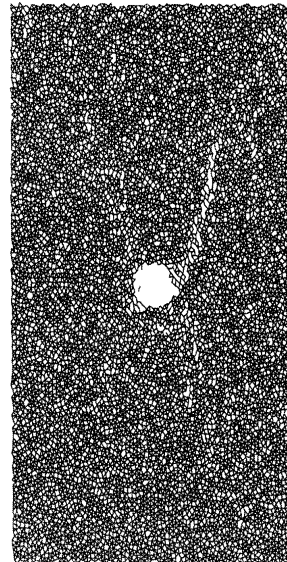
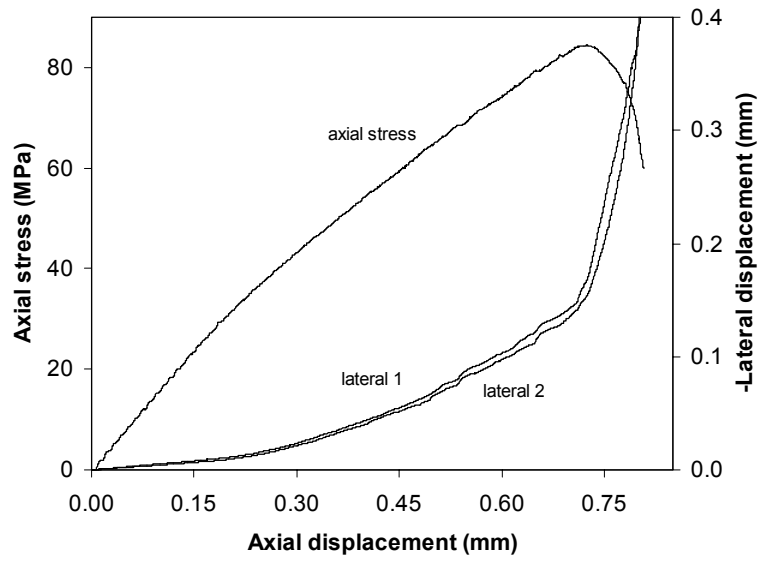


Figure 3. Numerical experiment. (a) Mechanical response. (b)-(e). Damage in specimen.